RSC Advances

ROYAL SOCIETY OF CHEMISTRY

www.rsc.org/advances

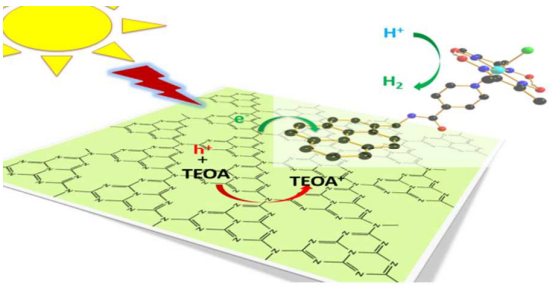

The pyrene-functionalized cobaloxime-g-C_3N_4 system was active for hydrogen production in CH_3CN-H_2O mixed solvent with a highest TON of 281.

Journal Name

RSCPublishing

ARTICLE

Efficient photocatalytic hydrogen evolution with end-group-functionalized cobaloxime catalysts in combination with graphite-like C_3N_4

Cite this: DOI: 10.1039/x0xx00000x

Received 00th January 2012,
Accepted 00th January 2012

DOI: 10.1039/x0xx00000x

www.rsc.org/

Xiao-Wei Song, [a] Hui-Min Wen, [a] Cheng-Bing Ma, [a] Hong-Hua Cui, [a] Hui Chen, [a] and Chang-Neng Chen*[a]

Three comparable hybrid photocatalytic systems, comprising semiconductor g-C_3N_4, end-group-functionalized cobaloxime complexes (carboxy-functionalized cobaloxime, **C1**; pyrene-functionalized cobaloxime, **C2**; and non-functionalized cobaloxime, **C3**), and triethanolamine (TEOA), are active for visible-light-driven hydrogen production in CH_3CN-H_2O (9/1, v/v) solution. Upon irradiation for 12 h, the turnover numbers of hydrogen evolution are 234, 281 and 195 for the hybrid system **C1**/g-C_3N_4, **C2**/g-C_3N_4 and **C3**/g-C_3N_4, respectively. The highest hydrogen evolution efficiency of the **C2**/g-C_3N_4 system can be attributed to the strongest π–π interactions between the pyrene moiety and g-C_3N_4. Based on electrochemical properties, steady-state photoluminescence spectra and theoretical analyses, the visible light absorption of g-C_3N_4, the catalytic H_2-evolving ability of cobaloxime as well as the efficient charge separation of the excited g-C_3N_4 in the presence of both TEOA and cobaloxime, are responsible for the high activity of these hybrid systems.

Introduction

The visible-light-driven hydrogen evolution from water is one of promising approaches to provide renewable and clean energy for the future.[1] Therefore, a number of hydrogen-evolving systems have been actively developed including homogeneous and heterogeneous photocatalytic systems in recent years.[1d, 2] Studies on the homogeneous catalysts for hydrogen production are mainly focused on the first-row transition metal complexes, such as [FeFe]-hydrogenase mimics,[3] cobalt and nickel complexes.[4] Among various catalysts, the cobaloxime has been widely investigated for photocatalytic hydrogen evolution due to their convenient preparation and good catalytic activities.[5] Many cobaloxime-based photocatalytic systems for hydrogen production have been constructed utilizing the noble-metal-based photosensitizers, such as ruthenium,[6] rhenium,[7] platinum,[8] and iridium-based organometallic complexes.[9] However, because of the high cost of noble-metal-based photosensitizers, chemists attempt to replace them with other chromophores made of earth-abundant elements, such as organic xanthene dyes,[10] metalloporphyrins,[11] and photoactive nanomaterials.[2b, 12]

To our knowledge, Eisenberg and co-workers have employed the xanthene dye derivatives (S or Se in place of O in the xanthene ring) in combination with the cobaloxime for the light-driven generation of hydrogen, and reported the highest turnover of 9000 (*vs.* organic dye).[10b] Besides the organic dyes, the metalloporphyrins were also introduced as the photosensitizers to couple with cobaloxime catalysts for efficient photoinduced hydrogen production[11a, 11c] Nevertheless, one of the inherent weaknesses of the utilized organic and organometallic photosensitizers is their instability upon long-term irradiation.[13] Recently, an increasing number of noble-metal-free nanomaterials have been used as the light absorber, such as TiO_2,[14] CdS,[13a] core/shell CdSe/ZnS QDs,[15] and graphite-like C_3N_4 (referred to hereafter as g-C_3N_4), which can link cobaloximes directly onto the surface and overcome the drawback of the poor stability of the organic and organometallic photosensitizers.[16]

Among various nanomaterials, the environmentally benign g-C_3N_4 is rightfully attracting increased attention owing to its relatively high stability and suitable electronic structure (E_g=2.7 eV, conduction band at -1.42 V and valence band at 1.28 V *vs.* Ag/AgCl) covering the water-splitting potentials.[17] However, g-C_3N_4 alone shows very poor photocatalytic activities for water reduction and relies on surface co-catalysts, which can accelerate the separation of photogenerated electron/hole and increase the photocatalytic performance of g-C_3N_4. The precedents for catalytic systems which combined g-C_3N_4 with a co-catalyst, such as platinum group metals and MoS_2,[18] do exist but it is only recently that Co- and Ni-based molecular catalysts

have been used as co-catalysts.[13b, 16] Herein, three comparable cobaloxime complexes (**C1**, **C2** and **C3**) (Fig. 1) are synthesized and studied as molecular co-catalysts for hydrogen generation from hybrid systems containing the photoactive g-C_3N_4 and triethanolamine (TEOA) as electron donor in acetonitrile aqueous solution. The results of photocatalysis experiments show that the TONs of hydrogen evolution are 234 and 281 (*vs*. complex) for the hybrid systems **C1**/g-C_3N_4 and **C2**/g-C_3N_4, respectively. In comparison, the photocatalytic activity of the non-functionalized complex **C3** (TON=195) is lower than that of the carboxy-functionalized complex **C1** and pyrene-functionalized complex **C2** under the same conditions. To better understand the difference of photocatalytic activities, the adsorption of the complexes to g-C_3N_4, the electrochemical properties and the steady-state photoluminescence properties are investigated and discussed in detail.

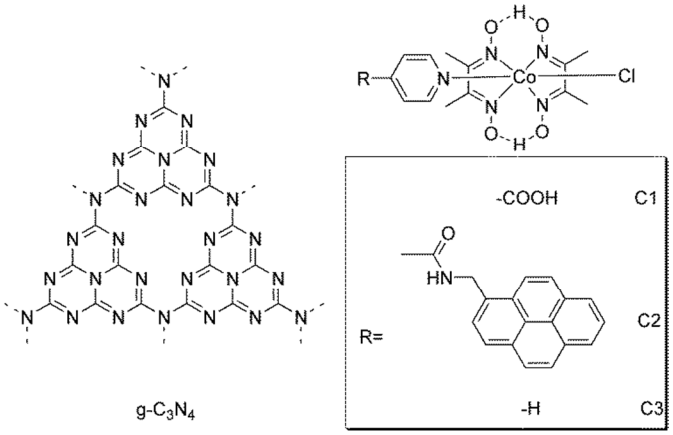

Fig. 1 Structures of g-C_3N_4 and complexes **C1** to **C3** used in the present work.

Result and discussion

Synthesis and structure of catalysts and g-C_3N_4

The g-C_3N_4 was prepared by the direct polymerization of urea at ambient conditions. The XRD pattern of the as-prepared g-C_3N_4 shows two characteristic peaks at 13.1 and 27.4 degree in accord with the previously reported results (Fig. S1†).[19] The TEM image clearly shows the g-C_3N_4 possesses the layered structure (Fig. S2†). In order to investigate the effect of end-group-functionalized cobaloximes on the photocatalytic performance of as-prepared g-C_3N_4, three cobaloxime complexes are designed as co-catalysts and expected to assemble on the surface of g-C_3N_4 for photocatalytic H_2 evolution. The first one (**C1**) is based on the relatively good adsorption performance of carboxy group, which can provide a linkage to the nanomaterial surface.[20] Furthermore, in view of the conjugative π structure of g-C_3N_4,[21] we choose another cobaloxime derivative **C2**, in which the pyrene moiety of π electron conjugation is expected to strongly interact with g-C_3N_4 via π–π interactions. As a comparison with the end-group-functionalized cobaloxime complexes **C1** and **C2**, the complex **C3** without functional-group modification is also employed as co-catalyst for g-C_3N_4 in this paper.

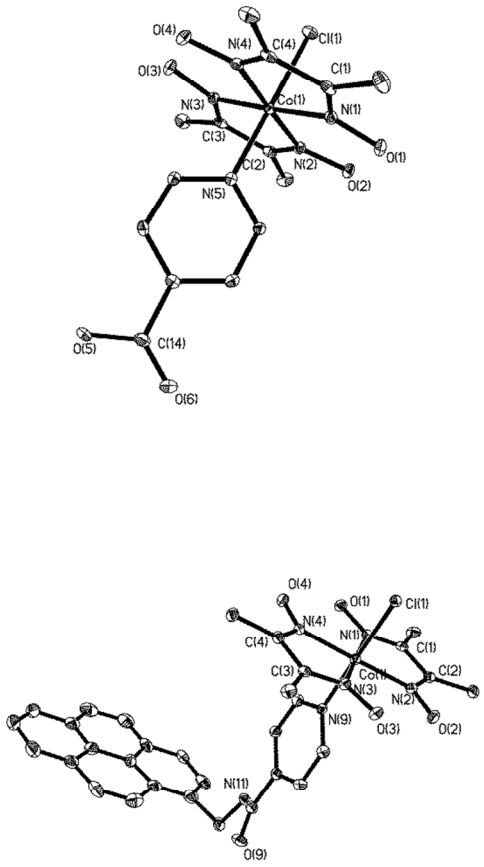

Fig. 2 Crystal structures of **C1** and **C2** (the hydrogen atoms are omitted for clarity)

The **C1** was conveniently prepared by stirring [Co(dmgH)(dmgH$_2$)Cl$_2$] with isonicotinic acid in CH_3CN and then obtained as dark-red crystals. The **C2** was prepared in an analogous manner to **C1** using [Co(dmgH)(dmgH$_2$)Cl$_2$] and N-pyren-1-ylmethyl-isonicotinamide, which was synthesized by the amidation reaction between isonicotinoyl chloride and (pyren-1-ylmethyl)amine. All new compounds were confirmed by ^1H, ^{13}C NMR and elemental analysis. The solid-state structures of **C1** and **C2** were established by means of single-crystal X-ray diffraction. The crystal structures of complexes **C1** and **C2** are given in Fig. 2 with selected bond lengths and angles listed in Table 1. The coordination geometry around the Co-centre in **C1** is strongly similar to those in other reported cobaloxime complexes.[8b] Because of the existence of the carboxyl, the axial Co-N(5)$_{pyridine}$ distance is 1.967 Å, slightly longer than that in **C3** (1.959 Å). The average Co-N$_{imine}$ bond distance of the glyoximate ligands in **C1** is 1.896 Å, which is consistent to the value of 1.895 Å in **C3**.[22] The asymmetric unit of **C2** consists of two same Co-centred complexes and some uncoordinated solvent molecules. For clarity, we only present one Co-centre in Fig. 2, which is hexacoordinated with a

slightly distorted octahedral geometry (Table 2). The pendent pyrene moiety is roughly parallel to the equatorial plane defined by the four N atoms of glyoximate ligands, with a dihedral angle of 5.6 degree.

Table 1 Selected bond lengths (Å) and angles (degree) for **C1** and **C2**

		C1	
Co(1)-N(1)	1.910(2)	N(3)-Co(1)-N(4)	98.64(10)
Co(1)-N(2)	1.887(2)	N(2)-Co(1)-N(4)	178.48(11)
Co(1)-N(3)	1.882(2)	N(3)-Co(1)-N(1)	177.92(11)
Co(1)-N(4)	1.906(2)	N(2)-Co(1)-N(1)	99.33(10)
Co(1)-N(5)	1.967(3)	N(4)-Co(1)-N(1)	80.26(11)
Co(1)-Cl(1)	2.2301(8)	N(3)-Co(1)-N(5)	89.63(10)
O(1)-N(1)	1.364(3)	N(2)-Co(1)-N(5)	89.41(10)
O(2)-N(2)	1.340(3)	N(4)-Co(1)-N(5)	92.07(10)
O(3)-N(3)	1.336(3)	N(1)-Co(1)-N(5)	92.17(10)
O(4)-N(4)	1.352(3)	N(3)-Co(1)-N(2)	81.72(10)
		C2	
Co(1)-N(1)	1.895(4)	N(3)-Co(1)-N(1)	177.37(18)
Co(1)-N(2)	1.904(4)	N(3)-Co(1)-N(4)	82.11(17)
Co(1)-N(3)	1.886(4)	N(1)-Co(1)-N(4)	98.27(17)
Co(1)-N(4)	1.898(4)	N(3)-Co(1)-N(2)	98.08(17)
Co(1)-N(9)	1.974(4)	N(1)-Co(1)-N(2)	81.48(17)
Co(1)-Cl(1)	2.2241(13)	N(4)-Co(1)-N(2)	178.84(17)
O(1)-N(1)	1.362(5)	N(3)-Co(1)-N(9)	90.92(17)
O(2)-N(2)	1.337(5)	N(1)-Co(1)-N(9)	91.68(17)
O(3)-N(3)	1.330(5)	N(4)-Co(1)-N(9)	90.07(15)
O(4)-N(4)	1.343(5)	N(2)-Co(1)-N(9)	91.07(16)

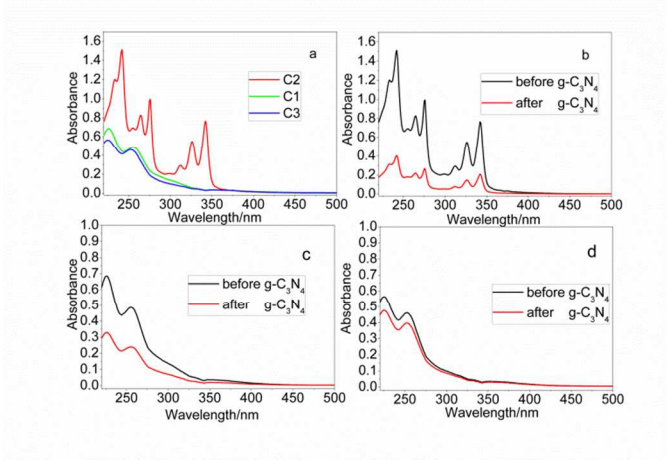

Fig. 3 (a) UV-vis absorption spectra of **C1** (2×10^{-5} M), **C2** (2×10^{-5} M) and **C3** (2×10^{-5} M) in CH_3CN (5 mL); UV-vis absorption spectra of **C2** (b), **C1** (c), and **C3** (d) before and after stirred with g-C_3N_4 (4 mg) in CH_3CN for 2 h following centrifugation and filtration.

Adsorption of the cobaloximes C1-C3 to g-C_3N_4

The UV-vis diffuses reflectance absorption spectrum of g-C_3N_4 exhibits the broad absorption from UV to visible light region (Fig. S4†). The absorption edge is at about 455 nm, corresponding to a small band-gap (2.73 eV). The UV-vis absorption spectra of complexes **C1-C3** measured in CH_3CN are shown in Fig. 3a. The cobaloximes **C1** and **C3** exhibit a high-energy absorption between 230 nm and 300 nm, which is attributed to the intra-ligand (π-π*) transitions.[8b] Unlike **C1** and **C3**, the **C2** displays a very different absorption spectrum with characteristic absorption bands of the pyrene group (at 342, 326, 312, 276, 265, 255, 242, and 235 nm).[23] According to the report by Li *et al*., the cobaloximes bearing appropriate pendent ligands can be effectively adsorbed by the photoactive nanomaterials.[13a] To investigate the adsorption amount of the cobaloximes **C1-C3** on the g-C_3N_4 surface, the acetonitrile solutions of **C1-C3** (2×10^{-5} M, 5 mL) were measured by UV-vis spectrophotometry before and after exposure to g-C_3N_4 (Fig. 3). In view of the absorbance difference at the maximum adsorption wavelength, we estimate the adsorption amount of **C1**, **C2**, and **C3** on g-C_3N_4 to be approximately 0.05, 0.07, and 0.02 μmol, respectively. Increasing the original concentration of cobaloximes from 2×10^{-5} M to 3×10^{-5} M did not lead to the increase in adsorption amount. As noted, however, no significant difference in the adsorption amount was seen between the above-mentioned cobaloximes, with a median adsorption amount for each of about 0.04 μmol.

Photocatalytic activities of the hybrid systems

We first studied the photocatalytic H_2 production of the hybrid system **C1**/g-C_3N_4 in CH_3CN-H_2O (9:1, v/v, 5 mL) solution containing 5 vol% TEOA at pH 10. Experiments under irradiation (λ>400 nm) with different concentration of **C1** (0.05-0.2 mM) showed the system with 0.1 mM **C1** released the largest amount of H_2 (42 μmol, TON = 84) over 4 h (Table 2). With an increase or a decrease of the concentration of **C1** to 0.2 mM and 0.05 mM, the TON of H_2 evolution decreased to 40 and 56, respectively. It is evident that the optimum amount (0.5 μmol) of **C1** for the system is much higher than the adsorption amount (0.05 μmol) of **C1** on the surface of g-C_3N_4, which indicates that the complex **C1** predominantly exists as free molecules in reaction solution. To further clarify the role of **C1**, the suspension of the **C1**/g-C_3N_4 system was stirred for 2 h in the dark and subsequently filtered, resulting in the g-C_3N_4 residue and the clear filtrate. With readdition of reaction solution, the g-C_3N_4 residue adsorbing a small amount of **C1** (0.05 μmol) gave a quarter of the TON of the original **C1**/g-C_3N_4 system, while with readdition of fresh g-C_3N_4, the clear filtrate containing the free molecules displayed an H_2 evolution rate similar to that of the original system **C1**/g-C_3N_4 (Fig. S6†). These results indicate that both of the **C1** molecules, adsorbed on the surface of g-C_3N_4 and dissolved in reaction solution, can improve the photocatalytic activities of g-C_3N_4. The light-induced H_2 production catalyzed by **C1** also depends on the amount of g-C_3N_4. When the concentration of **C1** was 0.1 mM, the amount of H_2 evolved was improved apparently with an increase of the amount of g-C_3N_4 from 2 mg to 4 mg. However, further increasing the amount of g-C_3N_4 to 8 mg did not lead to an obvious enhancement in the photocatalytic activity. Control experiments without **C1**, g-C_3N_4, or TEOA showed no H_2 was released from the system **C1**/g-C_3N_4, suggesting that all three components are required for the photocatalytic H_2 evolution.

Besides CH_3CN, CH_3CH_2OH and DMF were also used as reaction solvent for the photocatalytic experiment in the **C1**/g-C_3N_4 system. Smaller quantities of hydrogen were released in systems containing either CH_3CH_2OH or DMF, albeit with the same 9/1 v/v ratio with water (Fig. 4). Consequently, the solvent CH_3CN is superior to CH_3CH_2OH and DMF for H_2

evolution in this system. Further studies on solvent effects were done to investigate the photocatalytic activity of the system **C1**/g-C_3N_4 by changing the ratio of CH_3CN and H_2O. The results showed that the **C1**/g-C_3N_4 system displayed a higher activity when the CH_3CN/H_2O ratio was increased. With an increase of CH_3CN/H_2O ratio to 9/1 from 1/1, the TON of H_2 evolution was apparently increased to 88 from 10. In addition to the system **C1**/g-C_3N_4, the effects of the two factors (i.e., organic solvents and CH_3CN/H_2O ratios) on the photocatalytic performances in the analogous systems **C2**/g-C_3N_4 and **C3**/g-C_3N_4 were also studied in Fig. 4. It is found that the trends of the medium dependence on hydrogen evolution over the **C2**/g-C_3N_4 and **C3**/g-C_3N_4 systems agree closely with those over the **C1**/g-C_3N_4 system (Fig. 4).

Table 2 Influence of the concentration of **C1** and the amount of g-C_3N_4 on photocatalytic H_2 production [a]

Run	Concentration of **C1** (mM)	Amount of g-C_3N_4 (mg)	TON
1	0.05	4	56
2	0.1	4	84
3	0.2	4	40
4	0.1	2	57
5	0.1	8	92

[a] Condition: 5 vol% TEOA in CH_3CN-H_2O (9/1, v/v) at pH 10; irradiation time 4 h.

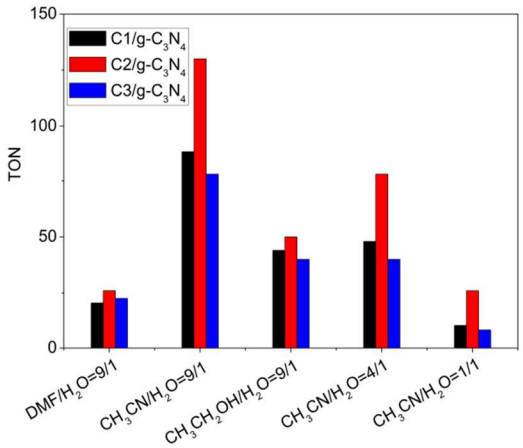

Fig. 4 Effects of organic solvents and CH_3CN/H_2O ratios on the hydrogen evolution over each system containing cobaloxime (1×10^{-4} M), g-C_3N_4 (4 mg) and TEOA (5 vol%) at pH 10; irradiation time 6 h.

Considering the aforementioned catalytic condition, the pH value of the **C1**/g-C_3N_4 system is approximately 10 without any adjustment by acid or base. To examine the pH effects on H_2 evolution from the system **C1**/g-C_3N_4, light-induced H_2 evolution was performed in the pH range of 8.5-10 under the conditions described in Fig. 5. The results show that the photocatalytic H_2 production is dependent on the pH value of the system, in which the optimum pH value for H_2 evolution is 9, while lower amounts of H_2 are obtained at either lower or higher pH values. The mechanism on the similar pH-dependent phenomenon has been elucidated in more detail by Zhang *et al.*[10c] In addition, the pH dependence on hydrogen production over the systems **C2**/g-C_3N_4 and **C3**/g-C_3N_4 also shows that the maximum hydrogen generation efficiency was achieved at pH 9. This pH-dependent effect is related to the oxidation of TEOA, which is an essential step in the catalytic cycle.[8a] As we know, TEOA is extensively used as electron donor in many Pt/g-C_3N_4-based hydrogen evolution systems.[19a, 21a, 24] In the **C1**/g-C_3N_4 system, keeping the concentration of **C1** (1×10^{-4} M) and the amount of g-C_3N_4 (4mg) unchanged, increasing the concentration of TEOA from 2.5 to 5 vol% apparently improved the efficiency of H_2 production. Further increasing the concentration of TEOA to 10 vol%, however, led to no obvious increase in the amount of H_2 production (Fig S9†). As a result, an optimized H_2 evolution system containing 1×10^{-4} M **C1**, 4 mg g-C_3N_4, and 5 vol% TEOA in 5 mL CH_3CN-H_2O (9/1, v/v) at pH 9.0 was able to photocatalyze H_2 evolution with a TON of 234.

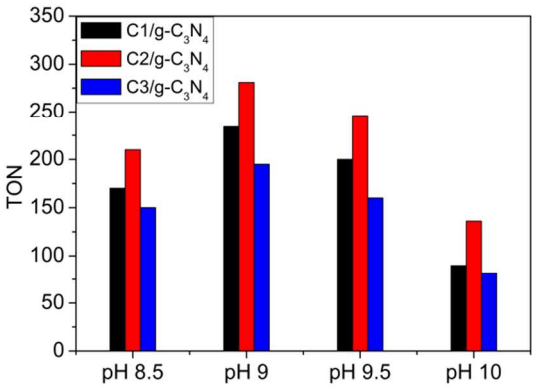

Fig. 5 pH dependence on the hydrogen production over each system under the following conditions: TEOA (5 vol%), cobaloxime (1×10^{-4} M) and g-C_3N_4 (4 mg) in CH_3CN-H_2O (9/1, v/v) solution; irradiation time 12 h.

To examine the effect of carboxyl group on the photocatalytic activity, the photocatalytic H_2 production experiment by the **C3**/g-C_3N_4 system was studied under the same conditions. A total amount of evolved H_2 reached 97 μmol, corresponding to a TON of 195. The activity of the **C1**/g-C_3N_4 system is higher than that of the **C3**/g-C_3N_4 system, indicating that the carboxy group functions satisfactorily as a linkage for H_2 evolution. Furthermore, it was found that the **C2**/g-C_3N_4 system displayed the highest activity among these three complexes, with TONs up to 281(Fig. 6). As expected, both of the **C2** molecules, adsorbed on g-C_3N_4 and dissolved in solution, also displayed the highest H_2 evolution efficiency among three (Fig S7†). These results indicate that the **C2** is the best co-catalyst for H_2 production in the current photocatalytic system, presumably due to π-π interactions between **C2** and g-C_3N_4.

The photocatalytic H_2 production of the **C1**/g-C_3N_4 system leveled out after 9 h of irradiation (Fig. 6). To investigate the reason(s) for the cease of H_2 generation, after the photocatalysis reaction, the suspension was filtered and the separated solid

was washed with water and dried in vacuum. The UV-vis absorption spectrum of the resulting clear solution is different from that of the original **C1** (Fig. S5†). Thus we speculate that the cessation of H_2 production may be ascribed to the degradation of **C1**. Besides the degradation of **C1** after photocatalysis reaction, the pH value of system changed to 9.6 from 9 after photocatalytic process. After 12 h of irradiation, to recover H_2 evolution of the **C1**/g-C_3N_4 system, the photocatalytic experiment with readdition of **C1** (0.5 μmol) to the system showed a recovered but lowered activity for hydrogen evolution under irradiation (Fig. S10†). For comparison, $CoCl_2$ was also tested for the photocatalytic H_2 evolution with g-C_3N_4 under the same conditions. The results show that the photocatalytic activity of the $CoCl_2$/g-C_3N_4 system is fairly lower than that of the **C1**/g-C_3N_4 system (Fig. S11†), suggesting that the active species in the current system is the cobaloxime **C1** rather than the decomposed products. The TEM image of the separated solid is as shown in Fig. S3, which is similar to the TEM image before irradiation, indicating that g-C_3N_4 is stable in the photocatalytic process. No zero-valent cobalt colloids were observed in the TEM image, which further proved the active species is also not the zero-valent cobalt in this system. The XRD pattern of the isolated solid is very similar to that of the freshly prepared g-C_3N_4, except for a decrease in the intensity of the peak at 27.4 degree (Fig. S1†).

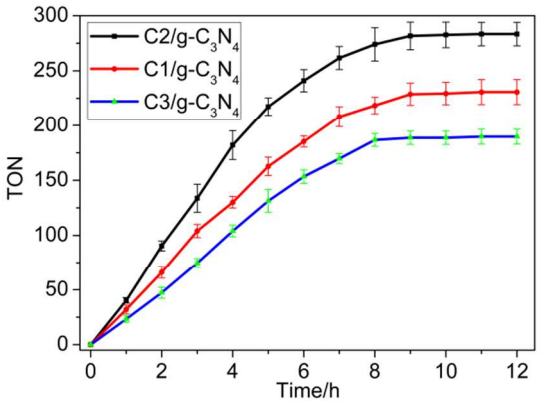

Fig. 6 Time dependence of hydrogen production using different cobaloxime complexes **C1** to **C3** (1×10^{-4} M) under the following conditions: g-C_3N_4 (4 mg) and TEOA (5 vol%) in CH_3CN-H_2O (9/1, v/v) solution (5 mL) at pH 9, error bars represent standard errors of the means of three independent experiments.

Electrochemical properties

The redox potential of the complexes is crucial to understand the electron transfer in photocatalytic process. Cyclic voltammetry studies were performed in CH_3CN with Bu_4NPF_6 as supporting electrolyte under N_2. The electrochemical reduction processes of **C1**-**C3** are shown in Fig. S12†. The reduction potentials are versus Fc^+/Fc and are summarized in Table 3. All Co^{III} complexes have two reductions, which can be assigned to Co^{III}/Co^{II} and Co^{II}/Co^{I}, respectively.[25] The first irreversible reduction potentials of **C1**, **C2** and **C3** are confirmed to be at about -1.06, -1.13, and -1.22 V, respectively. The first potentials of **C1** and **C2** are anodic shift relative to **C3**, which may be attributable to the axial pyridine ligand modified by electron-withdrawing group (-COOH or -CONH). But there is no above trend in the second potentials for Co^{II}/Co^{I} couple. The potentials at the secondary reduction are nearly equal for the three complexes. The behaviour of electrocatalytic proton reduction by **C1** or **C2** was studied by cyclic voltammograms in the presence of CH_3COOH (Fig. S13-S14†). Overall, complexes **C1** and **C2** behaved analogously toward electrocatalytic proton reduction.

Table 3 Electrochemical potentials [a] (vs. Fc^+/Fc) for all cobaloximes

Cobaloximes	Co^{III}/Co^{II} $E_{1/2}$ [b]	Co^{II}/Co^{I} $E_{1/2}$	ΔG [c]
C1	-1.06	-1.56	-0.31
C2	-1.13	-1.48	-0.39
C3	-1.22	-1.50	-0.37

[a]: electrochemical potentials were obtained by cyclic voltammetry studies under a N_2 atmosphere with 0.1 M Bu_4NPF_6 as the supporting electrolyte in CH_3CN. [b]: irreversible reduction wave. [c]: ΔG = the potential of CB(g-C_3N_4) - $E_{1/2}(Co^{II}/Co^{I})$, CB(g-C_3N_4) = -1.87 V

The probable mechanism on the photocatalytic H_2 production

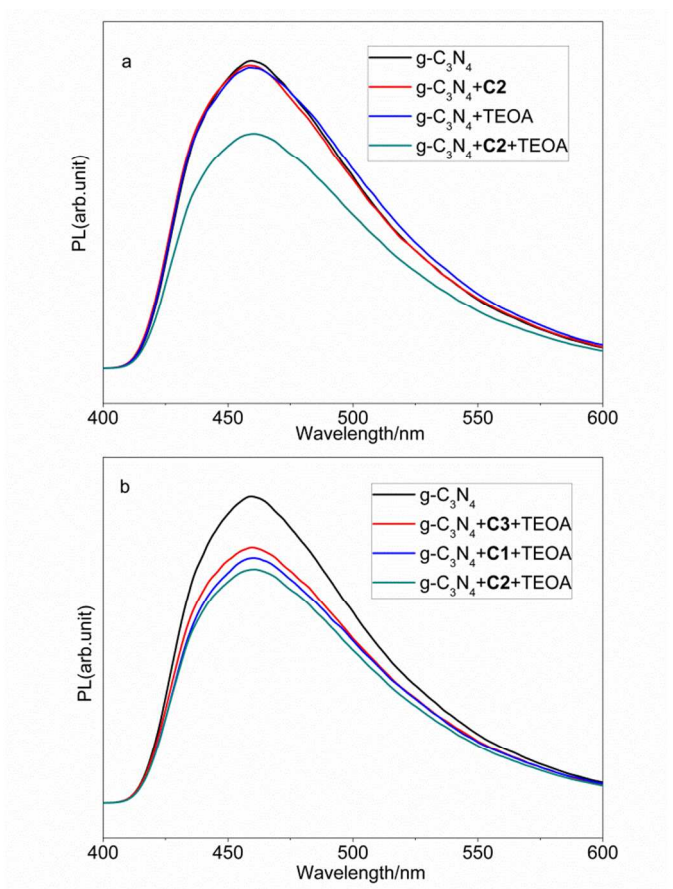

Fig. 7 (a) the emission spectra of g-C_3N_4 (0.8 g/L, 5 mL) suspension in CH_3CN-H_2O (9/1, v/v) solution at pH 9 in the presence of **C2** (1×10^{-4} M), TEOA (5 vol%), TEOA (5 vol%) and **C2** (1×10^{-4} M); (b) the fluorescence quenching of g-C_3N_4 in the presence of **C1** (1×10^{-4} M), **C2** (1×10^{-4} M), and **C3** (1×10^{-4} M) in 5 vol% TEOA acetonitrile aqueous solution.

The estimated reduction potential of g-C_3N_4 is -1.42 V relative to Ag/AgCl,[18a] which can be adjusted to -1.87 V versus Fc^+/Fc (E^0 of Fc^+/Fc = 0.45 V vs. Ag/AgCl).[26] The reduction potentials of the catalysts **C1**-**C3** are given in Table 3. According to Weller-equation, the values of free-energy changes (ΔG) for formation of Co^I species are determined to be -0.31, -0.39, and -0.37 V for each system, respectively (Table 3). The negative ΔG suggests that it is thermodynamically feasible for photoinduced electron transfer from the conduction band of g-C_3N_4 to these catalysts. However, there is no significant difference in the ΔG value between the three hybrid systems.

To explore the charge transfer pathways, the steady-state photoluminescence properties of the **C2**/g-C_3N_4 system were investigated in acetonitrile aqueous solution. The g-C_3N_4 suspension excited at 375 nm results in a maximal fluorescence emission peak at 459 nm (Fig. 7a). No significant decreases in fluorescence intensity are observed upon addition of either **C2** or TEOA. The reason for this phenomenon may plausibly be attributed to the fast recombination of photogenerated electron/hole pairs. However, a larger fluorescence quenching of g-C_3N_4 by 25% upon addition of both TEOA and **C2** is observed, suggesting that both **C2** and TEOA are required for the separation of the photogenerated electron/hole. Based on hydrogen production experiment and the above spectroscopic study, a plausible pathway of the photocatalytic H_2 evolution reaction is proposed in Fig. 8. Under visible light irradiation, the excited state electrons of the valence band of g-C_3N_4 would transport to the conduction band. The conduction-band electron of g-C_3N_4 can give two electrons to **C2** to form to Co^I species. The photogenerated Co^I species is protonated to obtain a Co-H intermediate, which finally reacts with another proton to generate H_2.[5a] Meanwhile the electron donor TEOA is oxidized by the photogenerated holes in the valence band.

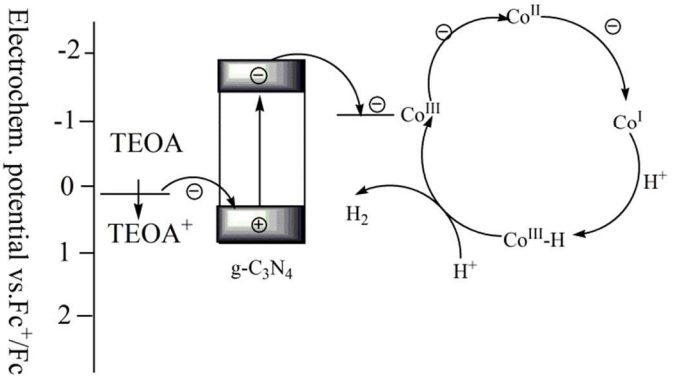

Fig. 8 A proposed pathway for the photocatalytic H_2 evolution by cobaloxime-g-C_3N_4 systems.

In contrast, the fluorescence intensity of g-C_3N_4 decreased by 20% and 14% upon addition of **C1**+TEOA and **C3**+TEOA (Fig. 7b), respectively. The sequence of the effectiveness quenching fluorescence of g-C_3N_4 is **C2** > **C1** > **C3**, which corresponds to the order of their photocatalytic H_2 evolution activity. According to previous reports on hybrid photocatalytic systems containing cobaloxime, the photocatalytic activity could be influenced by the adsorption amount of cobaloximes on nanomaterials, the driving force (ΔG) of electron transfer and the attachment mode between cobaloxime and nanomaterials.[13a, 14a, 15-16] However, no apparent difference in terms of the adsorption amount and the driving force was found between the present three systems. Therefore, the reason for the activity difference may be attributed to the attachment mode between g-C_3N_4 and cobaloximes. Compared with the free-collision mode between the non-functionalized **C3** and g-C_3N_4, the direct attachment (i.e., carboxy linkage or π-π interactions) between end-group functionalized cobaloxime and g-C_3N_4 could promote the charge transfer from g-C_3N_4 to the co-catalytic centres.

Conclusions

Three end-group-functionalized cobaloxime complexes as co-catalyst were designed and assembled on the surface of g-C_3N_4 for photocatalytic H_2 evolution in CH_3CN-H_2O (9/1, v/v) solution at pH 9. The photocatalytic experiments gave the highest TON of 234, 281 and 195 for **C1**/g-C_3N_4, **C2**/g-C_3N_4 and **C3**/g-C_3N_4 hybrid systems, respectively. The photocatalytic activity of these systems was attributed to the efficient charge separation of the excited g-C_3N_4, which was proved by steady-state photoluminescence spectra. Among the cobaloximes, the **C2** was superior to **C1** and **C3** as co-catalyst for H_2 production, which may result from the π-π interactions between **C2** and g-C_3N_4. Due to the degradation of cobaloxime, the catalytic lifetime of the hybrid system is short, which motivates us to seek more stable and effective molecule co-catalysts for g-C_3N_4.

Experimental section

Chemicals

All chemicals in this work were purchased from commercial sources and used without further purification. (pyren-1-ylmethyl)amine,[27] complexes [Co(dmgH) ($dmgH_2$)Cl_2],[28] and [Co($dmgH)_2$pyCl] (**C3**)[28] were synthesized according to previously described procedures.

Synthesis

The preparation of g-C_3N_4 was following a previously reported method.[19] Briefly, 10 g dry urea was added to an alumina crucible with a cover under ambient pressure in air. The precursor was put in a muffle furnace and heated to 550°C in 2 h and maintained at this temperature for 3 h. The obtained powders were rinsed several times with distilled water and ethanol and dried in vacuum at 80°C for 8 h.

N-pyren-1-ylmethyl-isonicotinamide. A mixture of isonicotinic acid (0.30 g, 2.44 mmol) and thionyl chloride (20 mL) in a round-bottomed flask was refluxed for 5 h with stirring. Excess thionyl chloride was removed under reduced pressure until yellow powders of isonicotinoyl chloride were obtained. A solution of the prepared isonicotinoyl chloride in 20 ml of CH_2Cl_2 was treated with a mixed solution of (pyren-1-ylmethyl)amine (0.46 g, 2.00 mmol) and triethylamine (3 mL)

in 20 ml of CH_2Cl_2 with vigorous stirring at 0°C. After addition, the resulting mixture was allowed to react for another 8 h at room temperature. Finally, the solvent was evaporated, and the residue was purified by chromatography on a silica gel column. Elution with CH_3OH-CH_2Cl_2 (1:5, v/v) furnished pure N-pyren-1-ylmethyl-isonicotinamide (0.61 g, 91%). Anal. Calcd for $C_{23}H_{16}N_2O$: C, 82.12%; H, 4.79%; N, 8.33%. Found: C, 82.09%; H, 4.81%; N, 8.29%. ^{1}H NMR (400 MHz, $CDCl_3$) δ 8.64 (2 H, d, J=5.4 Hz), 8.27 (1 H, d, J=9.2 Hz), 8.24–8.19 (2 H, m), 8.16 (2H, d, J=8.6 Hz), 8.05 (4 H, dt, J=16.9 Hz, 8.7 Hz), 7.58 (2 H, d, J= 5.6 Hz), 6.63 (1 H, s), 5.34 (2 H, d, J=5.1 Hz). ^{13}C NMR (101 MHz, $CDCl_3$) δ 165.06, 150.28, 141.50, 131.55, 131.23, 130.68, 130.06, 129.19, 128.64, 127.85, 127.49, 127.31, 126.28, 125.67, 125.56, 125.11, 124.86, 124.66, 122.51, 120.97, 42.80.

[Co(dmgH)$_2$(4-COOH-py)Cl] (**C1**). A 0.36 g (1.00 mmol) sample of [Co(dmgH)(dmgH$_2$)Cl$_2$] was suspended in 40 ml of CH_3CN. One equivalent of isonicotinic acid (0.12 g, 1.00 mmol) was then added to the flask and heated at 70 °C with stirring for 1 h. The resulting dark-red solution was filtered and left overnight. Dark-red crystals (0.39 g, 87%) of suitable for X-ray analysis were obtained. Anal. Calcd for $CoClC_{14}N_5O_6H_{19}\cdot H_2O$: C, 36.10%; H, 4.54%; N, 15.04%. Found: C, 36.47%; H, 4.44%; N, 15. 16%. ^{1}H NMR (400 MHz, CD_3CN) δ 8.30 (2H, d, J = 6.8 Hz), 7.72 (2H, d, J = 6.7 Hz), 2.31 (12H, s).

[Co(dmgH)$_2$(N-pyren-1-ylmethyl-isonicotinamide)Cl] (**C2**). Triethylamine (0.10 g, 1.00 mmol) was added to a stirred, green suspension of [$CoCl_2$(dmgH)(dmgH2)] (0.36 g, 1.00 mmol) in CH_3OH (25 mL), resulting in a brown solution. A solution of N-pyren-1-ylmethyl-isonicotinamide (0.33 g, 1.00 mmol) in 15 ml of CH_2Cl_2 was added after five minutes and the reaction mixture was heated at 40 °C for 1 h. The resulting brown solution was filtered and left overnight. Brown crystals (0.50 g, 76%) of suitable for X-ray analysis were obtained. Anal. Calcd for $CoClC_{31}N_6O_5H_{30}$: C, 56.33%; H, 4.57%; N, 12.71%. Found: C, 56.47%; H, 4.62%; N, 12.60%. ^{1}H NMR (400 MHz, $CDCl_3$) δ 8.32 (2 H, d, J=4.8 Hz), 8.22 (3 H, d, J=7.8 Hz), 8.14 (2 H, d, J=9.2 Hz), 8.11–8.00 (3 H, m), 7.98 (1 H, d, J=7.4 Hz), 7.55 (2 H, d, J=4.8 Hz), 6.71 (1 H, s), 5.30 (2 H, s), 2.31 (12 H, s).

Adsorption experiments: a solution of **C1**, **C2** or **C3** (2×10^{-5} M, 5 ml) in CH_3CN solution was added to g-C_3N_4 (4 mg) in a schlenk tube. The mixture was stirred for 2 h in the dark and subsequently centrifuged. The filtered, clear solution was then measured by UV–visible absorption spectra. The amount of **C1**, **C2** or **C3** adsorbed on g-C_3N_4 was estimated by the absorbance difference at the absorption peak before and after adsorption on to g-C_3N_4.

Physical measurements

Elemental analyses were carried out on a Vario MICRO Elemental Analyser. ^{1}H，^{13}C NMR spectra were performed on a Bruker Avance III (400 MHz) spectrometer. TEM analyses were conducted on a JEM-2010 electron microscope at an acceleration voltage of 200 kV. UV-Vis absorption spectra were measured on a Perkin-Elmer Lambda 35 UV-Vis spectrophotometer.

X-ray diffraction

X-Ray single-crystal data of **C1** and **C2** were collected on a SuperNova, Dual, Cu at zero, Atlas diffractometer. Crystal data collection, refinement and reduction were accomplished with the CrysAlisPro, Agilent Technologies, Version 1.171.36.28. The crystal structures were solved by direct methods with SHELXS-97 and refined by using the SHELXL-97 crystallographic software package. All non-hydrogen atoms were refined anisotropically. The hydrogen atoms were added in a riding model. Details of crystal data are summarized in Table 4. CCDC-955344 and CCDC-982938 (for **C1** and **C2**) contain the supplementary crystallographic data for this paper. Copies of the data can be obtained free of charge from The Cambridge Crystallographic Data Centre via www.ccdc.cam.ac.uk/data_request/cif. X-ray diffraction (XRD) was used to identify the structure of the g-C_3N_4 before and after photocatalytic reactions. Diffraction date were collected on a MiniFlex II diffractometer with Cu Kα radiation(30 KV×15 mA).The 2θ scanning range was from 10 degree to 50 degree with a scanning speed of 4 degree per min.

Table 4 Crystal data and structure refinement details for complex **C1** and **C2**

Complex	**C1**·(H_2O)(CH_3CN)	**C2**·(CH_3OH)(H_2O)$_2$(CH_2Cl_2)
Molecule formula	$C_{16}H_{24}ClCoN_6O_7$	$C_{64}H_{70}Cl_4Co_2N_{12}O_{13}$
Formula weight	506.79	1474.98
T (K)	100.00(13)	100.0(2)
Crystal system	triclinic	Triclinic
Space group	P-1	P-1
a (Å)	7.9393(3)	9.5141(4)
b (Å)	11.3829(4)	17.4267(9)
c (Å)	13.7720(6)	20.3947(10)
α (°)	111.729(4)	75.820(5)
β (°)	101.772(3)	87.861(4)
γ (°)	99.800(3)	74.763(4)
V (Å^3)	1089.74(7)	3161.8(3)
Z	2	2
F(000)	524	1528
D_{calc} (g cm^{-3})	1.544	1.549
$R1$/$wR2$ ($I > 2\sigma(I)$)	0.0394/0.0860	0.0715/0.1822
$R1$/$wR2$ (all data)	0.0447/0.0883	0.0994/0.2066
Goodness of fit	1.084	1.032

Electrochemistry

Electrochemical measurements were made using a CH instrument Model 630A Electrochemical Workstation. The cyclic voltammetry experiments were conducted in acetonitrile solution containing 0.1 M ^{n}Bu$_4$NPF$_6$ as the supporting electrolyte under N_2. Glassy carbon and platinum wire were used as the working and counter electrodes, respectively, and the potential was measured against the Ag/AgCl reference electrode and reported relative to the internal reference of Fc^+/Fc = 0.00 V.

Photocatalysis

In a typical procedure, g-C_3N_4 (4 mg), **C1** (500 μL, 1 mM) and 5 vol% triethanolamine (TEOA) acetonitrile aqueous (9/1, v/v) solution were added to a Schlenck bottle. The mixture was magnetically stirred under N_2 atmosphere for 15 min. The system was freeze-pump-thaw degassed for three times and then warmed to room temperature prior to irradiation. The reaction solution was irradiated at 25 °C using a Xe lamp (300 W) with a cutoff filter (λ>400 nm). The gas phase of the reaction system was analyzed on a GC 7900 instrument with a 5 Å molecular sieve column, a thermal conductivity detector, and using N_2 as carrying gas. The amount of hydrogen generated was determined by the external standard method. Hydrogen dissolved in the solution was not measured and the slight effect of the hydrogen generated on the pressure of the Schlenk bottle was neglected for calculation of the volume of hydrogen gas.

Acknowledgements

The authors thank the National Natural Science Foundation China (grant numbers 21071145, 21101153, 21231003 and 21203195) for financial support.

Notes and references

[a] State Key Laboratory of Structural Chemistry, Fujian Institute of Research on the Structure of Matter, Chinese Academy of Sciences, Fuzhou, Fujian 350002, P. R. China;E-mail: *ccn@fjirsm.ac.cn*

† Electronic Supplementary Information (ESI) available: [Fig. S1 - Fig. S14]. See DOI: 10.1039/b000000x/

1. (a) N. S. Lewis and D. G. Nocera, *Proc. Natl. Acad. Sci. USA*, 2006, **103**, 15729-15735; (b) R. M. Navarro, M. C. Alvarez-Galvan, J. A. Villoria de la Mano, S. M. Al-Zahrani and J. L. G. Fierro, *Energy Environ. Sci.*, 2010, **3**, 1865-1882; (c) E. S. Andreiadis, M. Chavarot-Kerlidou, M. Fontecave and V. Artero, *Photochem Photobiol*, 2011, **87**, 946-964; (d) W. T. Eckenhoff and R. Eisenberg, *Dalton Trans.*, 2012, **41**, 13004-13021.
2. (a) A. Kudo, *Int. J. Hydrogen. Energ.*, 2007, **32**, 2673-2678; (b) P. D. Tran, L. H. Wong, J. Barber and J. S. C. Loo, *Energy Environ. Sci.*, 2012, **5**, 5902-5918; (c) V. Artero and M. Fontecave, *Chem. Soc. Rev.*, 2013, **42**, 2338-2356.
3. (a) M. Wang, L. Chen, X. Li and L. Sun, *Dalton Trans.*, 2011, **40**, 12793-12800; (b) F. Wang, W. G. Wang, H. Y. Wang, G. Si, C. H. Tung and L. Z. Wu, *ACS Catal.*, 2012, **2**, 407-416.
4. (a) S. Losse, J. G. Vos and S. Rau, *Coord. Chem. Rev.*, 2010, **254**, 2492-2504; (b) W. Zhang, J. Hong, J. Zheng, Z. Huang, J. Zhou and R. Xu, *J. Am. Chem. Soc.*, 2011, **133**, 20680-20683; (c) Z. Han, W. R. McNamara, M. S. Eum, P. L. Holland and R. Eisenberg, *Angew. Chem. Int. Ed.*, 2012, **51**, 1667-1670; (d) H. H. Cui, J. Y. Wang, M. Q. Hu, C. B. Ma, H. M. Wen, X. W. Song and C. N. Chen, *Dalton Trans.*, 2013, **42**, 8684-8691; (e) H. N. Kagalwala, E. Gottlieb, G. Li, T. Li, R. Jin and S. Bernhard, *Inorg. Chem.*, 2013, **52**, 9094-9101.
5. (a) V. Artero, M. Chavarot-Kerlidou and M. Fontecave, *Angew. Chem. Int. Ed.*, 2011, **50**, 7238-7266; (b) M. Wang, L. Chen and L. Sun, *Energy Environ. Sci.*, 2012, **5**, 6763-6778.
6. A. Fihri, V. Artero, M. Razavet, C. Baffert, W. Leibl and M. Fontecave, *Angew. Chem. Int. Ed.*, 2008, **120**, 574-577.
7. (a) B. Probst, M. Guttentag, A. Rodenberg, P. Hamm and R. Alberto, *Inorg. Chem.*, 2011, **50**, 3404-3412; (b) M. Guttentag, A. Rodenberg, R. Kopelent, B. Probst, C. Buchwalder, M. Brandstätter, P. Hamm and R. Alberto, *Eur. J. Inorg. Chem.*, 2012, **2012**, 59-64.
8. (a) P. Du, K. Knowles and R. Eisenberg, *J. Am. Chem. Soc.*, 2008, **130**, 12576-12577; (b) P. Du, J. Schneider, G. Luo, W. W. Brennessel and R. Eisenberg, *Inorg. Chem.*, 2009, **48**, 4952-4962.
9. A. Fihri, V. Artero, A. Pereira and M. Fontecave, *Dalton Trans.*, 2008, 5567-5569.
10. (a) T. Lazarides, T. McCormick, P. Du, G. Luo, B. Lindley and R. Eisenberg, *J. Am. Chem. Soc.*, 2009, **131**, 9192-9194; (b) T. M. McCormick, B. D. Calitree, A. Orchard, N. D. Kraut, F. V. Bright, M. R. Detty and R. Eisenberg, *J. Am. Chem. Soc.*, 2010, **132**, 15480-15483; (c) P. Zhang, M. Wang, J. Dong, X. Li, F. Wang, L. Wu and L. Sun, *The Journal of Physical Chemistry C*, 2010, **114**, 15868-15874; (d) J. Dong, M. Wang, P. Zhang, S. Yang, J. Liu, X. Li and L. Sun, *The Journal of Physical Chemistry C*, 2011, **115**, 15089-15096; (e) L. Gong, J. Wang, H. Li, L. Wang, J. Zhao and Z. Zhu, *Catal Commun*, 2011, **12**, 1099-1103; (f) T. M. McCormick, Z. Han, D. J. Weinberg, W. W. Brennessel, P. L. Holland and R. Eisenberg, *Inorg. Chem.*, 2011, **50**, 10660-10666.
11. (a) P. Zhang, M. Wang, C. Li, X. Li, J. Dong and L. Sun, *Chem. Commun.*, 2010, **46**, 8806-8808; (b) K. Peuntinger, T. Lazarides, D. Dafnomili, G. Charalambidis, G. Landrou, A. Kahnt, R. P. Sabatini, D. W. McCamant, D. T. Gryko, A. G. Coutsolelos and D. M. Guldi, *The Journal of Physical Chemistry C*, 2012, **117**, 1647-1655; (c) M. Natali, R. Argazzi, C. Chiorboli, E. Iengo and F. Scandola, *Chem. Eur. J.*, 2013, **19**, 9261-9271.
12. F. Wen and C. Li, *Acc. Chem. Res.*, 2013, **46**, 2355-2364.
13. (a) F. Wen, J. Yang, X. Zong, B. Ma, D. Wang and C. Li, *Journal of Catalysis*, 2011, **281**, 318-324; (b) J. Dong, M. Wang, X. Li, L. Chen, Y. He and L. Sun, *Chemsuschem*, 2012, **5**, 2133-2138.
14. (a) F. Lakadamyali and E. Reisner, *Chem. Commun.*, 2011, **47**, 1695-1697; (b) F. Lakadamyali, M. Kato, N. M. Muresan and E. Reisner, *Angew. Chem. Int. Ed.*, 2012, **51**, 9381-9384; (c) F. Lakadamyali, A. Reynal, M. Kato, J. R. Durrant and E. Reisner, *Chem. Eur. J.*, 2012, **18**, 15464-15475.
15. J. Huang, K. L. Mulfort, P. Du and L. X. Chen, *J. Am. Chem. Soc.*, 2012, **134**, 16472-16475.
16. S. W. Cao, X. F. Liu, Y. P. Yuan, Z. Y. Zhang, J. Fang, S. C. J. Loo, J. Barber, T. C. Sum and C. Xue, *Phys. Chem. Chem. Phys.*, 2013, **15**, 18363-18366.
17. X. Wang, K. Maeda, A. Thomas, K. Takanabe, G. Xin, J. M. Carlsson, K. Domen and M. Antonietti, *Nat Mater*, 2009, **8**, 76-80.
18. (a) J. Zhang, X. Chen, K. Takanabe, K. Maeda, K. Domen, J. D. Epping, X. Fu, M. Antonietti and X. Wang, *Angew. Chem. Int. Ed.*, 2010, **49**, 441-444; (b) X. H. Li, X. Wang and M. Antonietti, *Chem. Sci.*, 2012, **3**, 2170-2174; (c) Y. Hou, A. B. Laursen, J. Zhang, G. Zhang, Y. Zhu, X. Wang, S. Dahl and I. Chorkendorff, *Angew. Chem. Int. Ed.*, 2013, **52**, 3621-3625.
19. (a) S. Min and G. Lu, *The Journal of Physical Chemistry C*, 2012, **116**, 19644-19652; (b) Y. Zhang, J. Liu, G. Wu and W. Chen, *Nanoscale*, 2012, **4**, 5300-5303.

20. (a) M. Sykora, M. A. Petruska, J. Alstrum-Acevedo, I. Bezel, T. J. Meyer and V. I. Klimov, *J. Am. Chem. Soc.*, 2006, **128**, 9984-9985; (b) J. Huang, D. Stockwell, Z. Huang, D. L. Mohler and T. Lian, *J. Am. Chem. Soc.*, 2008, **130**, 5632-5633; (c) A. J. Morris-Cohen, M. T. Frederick, L. C. Cass and E. A. Weiss, *J. Am. Chem. Soc.*, 2011, **133**, 10146-10154.
21. (a) K. Takanabe, K. Kamata, X. Wang, M. Antonietti, J. Kubota and K. Domen, *Phys. Chem. Chem. Phys.*, 2010, **12**, 13020-13025; (b) Y. Wang, Z. Wang, S. Muhammad and J. He, *CrystEngComm*, 2012, **14**, 5065-5070.
22. S. Geremia, R. Dreos, L. Randaccio, G. Tauzher and L. Antolini, *Inorg. Chim. Acta.*, 1994, **216**, 125-129.
23. V. Georgakilas, K. Kordatos, M. Prato, D. M. Guldi, M. Holzinger and A. Hirsch, *J. Am. Chem. Soc.*, 2002, **124**, 760-761.
24. (a) X. Wang, K. Maeda, X. Chen, K. Takanabe, K. Domen, Y. Hou, X. Fu and M. Antonietti, *J. Am. Chem. Soc.*, 2009, **131**, 1680-1681; (b) Y. Zheng, J. Liu, J. Liang, M. Jaroniec and S. Z. Qiao, *Energy Environ. Sci.*, 2012, **5**, 6717-6731.
25. M. Razavet, V. Artero and M. Fontecave, *Inorg. Chem.*, 2005, **44**, 4786-4795.
26. G. A. N. Felton, C. A. Mebi, B. J. Petro, A. K. Vannucci, D. H. Evans, R. S. Glass and D. L. Lichtenberger, *J. Organomet. Chem.*, 2009, **694**, 2681-2699.
27. H. Lee, E. Luna, M. Hinz, J. J. Stezowski, A. S. Kiselyo and R. G. Harvey, *J. Org. Chem.*, 1995, **60**, 5604-5613.
28. W. C. Trogler, R. C. Stewart, L. A. Epps and L. G. Marzilli, *Inorg. Chem.*, 1974, **13**, 1564-1570.